Discover Oncology

Analysis

The role of KLF5 in gut microbiota and lung adenocarcinoma: unveiling programmed cell death pathways and prognostic biomarkers

Qingliang Fang[1,2] · Meijun Xu[3] · Wenyi Yao[4] · Ruixin Wu[5] · Ruiqin Han[6] · Satoru Kawakita[7] · Aidan Shen[7] · Sisi Guan[1] · Jiliang Zhang[8] · Xiuqiao Sun[1] · Mingxi Zhou[1] · Ning Li[5] · Qiaoli Sun[1,10] · Chang-Sheng Dong[1,2,9]

Received: 4 July 2024 / Accepted: 20 August 2024
Published online: 05 September 2024
© The Author(s) 2024 OPEN

Abstract
Lung adenocarcinoma (LUAD) is the most important subtype of lung cancer. It is well known that the gut microbiome plays an important role in the pathophysiology of various diseases, including cancer, but little research has been done on the intestinal microbiome associated with LUAD. Utilizing bioinformatics tools and data analysis, we identified novel potential prognostic biomarkers for LUAD. To integrate differentially expressed genes and clinical significance modules, we used a weighted correlation network analysis system. According to the Peryton database and the gutMGene database, the composition and structure of gut microbiota in LUAD patients differed from those in healthy individuals. LUAD was associated with 150 gut microbiota and 767 gut microbiota targets, with Krüppel-like factor 5 (KLF5) being the most closely related. KLF5 was associated with immune status and correlated well with the prognosis of LUAD patients. The identification of KLF5 as a potential prognostic biomarker suggests its utility in improving risk stratification and guiding personalized treatment strategies for LUAD patients. Altogether, KLF5 could be a potential prognostic biomarker in LUAD.

Qingliang Fang, Meijun Xu and Wenyi Yao share the first authorship.

Supplementary Information The online version contains supplementary material available at https://doi.org/10.1007/s12672-024-01257-w.

✉ Qiaoli Sun, sunny5sunny@163.com; ✉ Chang-Sheng Dong, csdong@shutcm.edu.cn | [1]Longhua Hospital, Shanghai University of Traditional Chinese Medicine, No.725, Wanping Rd, Shanghai 200032, China. [2]Department of Oncology, Longhua Hospital, Shanghai University of Traditional Chinese Medicine, No.725, Wanping Rd, Shanghai 200032, China. [3]Acupuncture and Moxibustion Department, Affiliated Hospital of Jiangxi University of Traditional Chinese Medicine, Nanchang 330006, Jiangxi Province, China. [4]Department of Oncology II, Seventh People's Hospital of Shanghai University of Traditional Chinese Medicine, Shanghai 200137, China. [5]Preclinical Department, Shanghai Municipal Hospital of Traditional Chinese Medicine, Shanghai University of Traditional Chinese Medicine, No.274, Zhijiang Road, Jing'an District, Shanghai 200071, China. [6]State Key Laboratory of Common Mechanism Research for Major Diseases, Institute of Basic Medical Sciences, Chinese Academy of Medical Sciences and Peking Union Medical College, Beijing 100005, China. [7]Terasaki Institute for Biomedical Innovation, Los Angeles, CA 90024, USA. [8]Beijing Tong Ren Tang Chinese Medicine Co., LTD, Hong Kong 999077, China. [9]Cancer Institute of Traditional Chinese Medicine, Longhua Hospital, Shanghai University of Traditional Chinese Medicine, No.725, Wanping Rd, Shanghai 200032, China. [10]Teaching Department, Longhua Hospital, Shanghai University of Traditional Chinese Medicine, No.725, Wanping Rd, Shanghai 200032, China.

Graphical Abstract

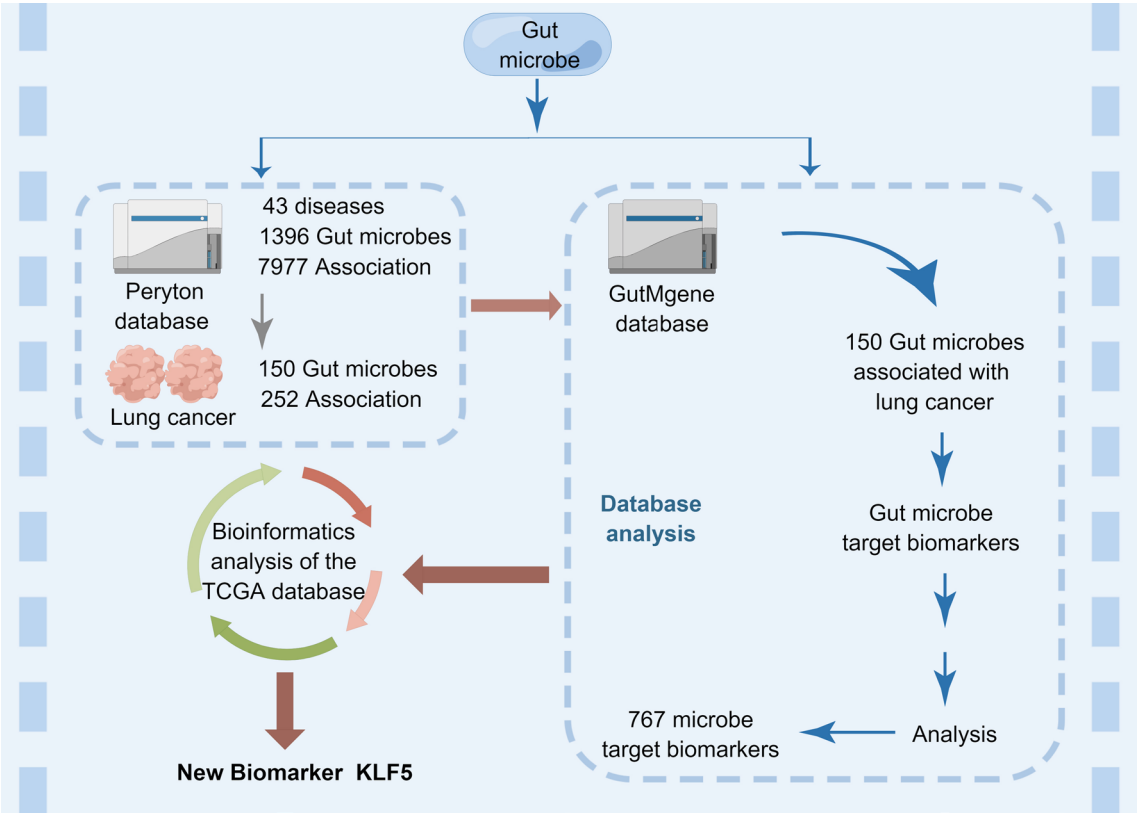

Keywords Gut microbiota · Biomarkers · Intestinal mucosal-related cancer · Lung adenocarcinoma · KLF5

1 Introduction

Lung cancer has the highest mortality rate among various types of cancers, reaching 21% [1, 2]. The mortality and incidence of Lung adenocarcinoma (LUAD), a subtype of lung cancer, are on the rise, threatening the health of LUAD patients. Early diagnostics is a key to successful treatment of the disease; however, it is hindered by current diagnosis limitations for LUAD [3, 4]. In order to improve early diagnosis, risk assessment, and prediction of treatment efficacy and recurrence of LUAD, it is essential to identify potent prognostic biomarkers, which have been explored in great detail [5]. Recent study of gut microbiota has revealed new biomarkers for LUAD in light of its significant role in cancer progression. By influencing metabolic pathways, suppressing immune cell function, and generating pro-inflammatory factors, the gut microbiota promotes the occurrence and advancement of lung cancer [6–9].

The "gut-lung axis" encompasses various communication pathways. This mechanism involves the cyclic transportation of soluble microbial components and metabolites, as well as the direct migration of immune cells from the gut to the respiratory tract through the bloodstream, such as ILC2s [10, 11]. The gut-lung axis suggests that the gut microbiota can affect lung health and disease, including cancer, through immune modulation and metabolic interactions. By modulating metabolic pathways, suppressing immune cell function, and producing pro-inflammatory factors, the gut microbiota plays a crucial role in cancer progression, promoting the development of lung cancer [6–8, 12]. Understanding this connection is crucial for identifying new therapeutic targets and prognostic markers, which may play a role in mediating these interactions.

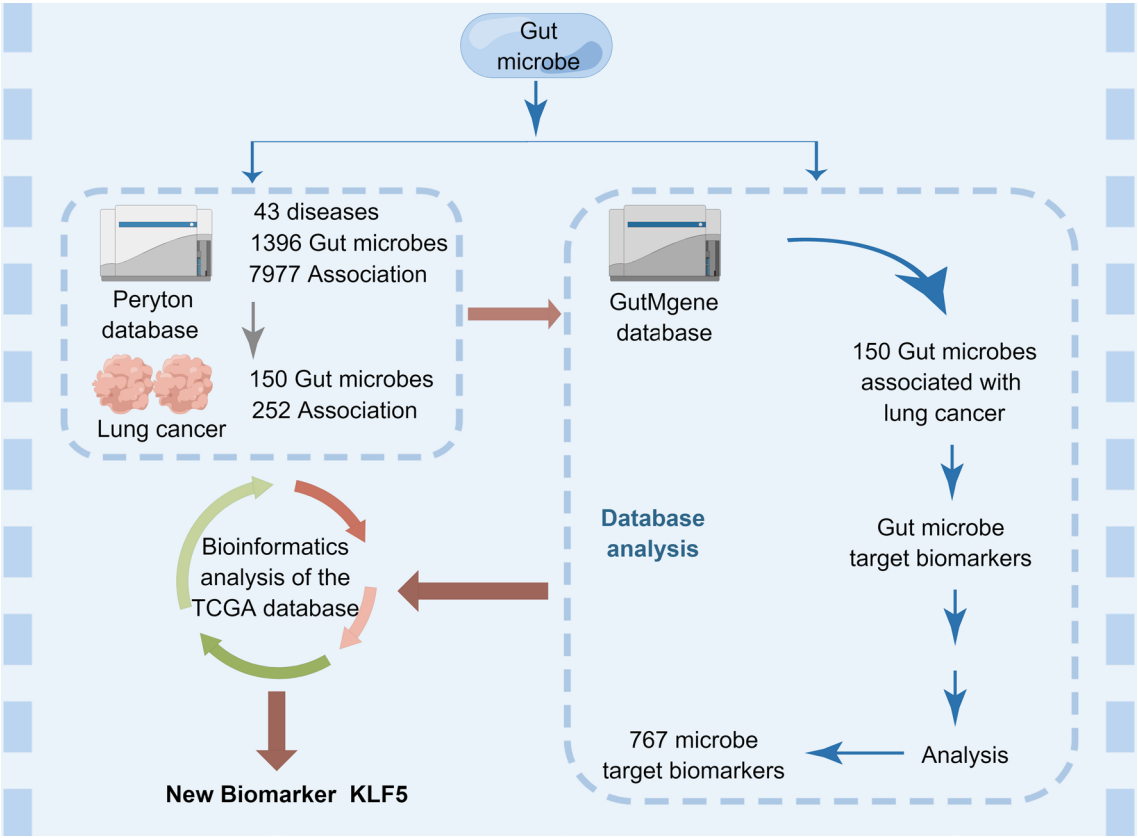

Fig. 1 The diagram shows the relationship between gut microbiome, lung cancer, and KLF5 based on the one health framework

Furthermore, infections are prevalent among cancer patients, and antibiotics are often administered to prevent and treat bacterial infections. Unfortunately, this may lead to drug-resistant infections. Gut microbiota dysbiosis (an imbalance of normal content) and antibiotic resistance appear to be involved in the growth of LUAD, primarily through the host's immune system. Additionally, microbial effects on dietary energy acquisition, the production of short-chain fatty acids, and antigenic mimicry with cancer cells contribute to these processes. In preclinical models, microbial metabolites can also influence the phenotype of tumor somatic mutations [6]. Hence, the gut microbiota, its metabolites, and the genes they target hold potential as markers for lung cancer.

KLF5 is a zinc finger transcription factor that plays a pivotal role in regulating cell proliferation, differentiation, and programmed cell death [13]. It has garnered attention for its complex and dual role in various cancers, functioning as both a tumor suppressor and promoter, depending on the context. In several cancers, such as breast [14], prostate [15], and bladder cancers [16], KLF5 is associated with increased tumor cell proliferation, invasiveness, and malignancy. Conversely, in colorectal cancer, loss or dysfunction of KLF5 contributes to cancer progression, highlighting its context-dependent roles [17]. However, there is a relative lack of in-depth research on KLF5 in LUAD, especially in the relationship between connecting microorganisms, such as gut microbiota, and LUAD, which has yet to be explored.

In our research on the relationship between gut microbiota and LUAD, we collected a total of 150 gut microbes from the Peryton database and GutMgene database. Among these microbes, we identified 767 microbe target biomarkers. To identify the biomarkers most closely associated with lung cancer, we performed bioinformatics analysis using the Cancer Genome Atlas Program (TCGA) database. Our analysis led us to conclude that KLF5 could serve as a potential prognostic biomarker for LUAD (Fig. 1). The objective of this study was to investigate the correlation between gut microbiota, KLF5 expression, and lung cancer through bioinformatics analysis. We examined the expression levels and

immune mechanisms of KLF5 in LUAD and assessed its association with patient survival. Our findings may contribute to the development of a novel gut microbiota-related marker for predicting survival and prognosis in LUAD patients.

2 Materials and methods

2.1 Data collection

All microbial data were obtained from the Peryton database [18] and GutMGene databases [19]. The Peryton database contains experimentally validated associations between microbes and diseases, while the GutMGene database provides manually curated information on microbe-metabolite, microbe-target, and metabolite-target relationships in humans and mice. These relationships were extracted from nearly 400 publications and have been experimentally validated in vivo or in vitro using techniques such as RT-qPCR, high-performance liquid chromatography, and 16S rRNA-seq.

All mRNA transcriptome data and associated clinical information for LUAD were retrieved from the publicly available TCGA database (https://www.cancer.gov/). The mRNA expression data were collected from a total of 347 adjacent tissue samples and 515 cancer tissue samples. Pan-cancer RNA-seq data from TCGA, TOIL, and GTEx were obtained from the UCSC XENA platform (https://xenabrowser.net/datapages/) [20]. The clinical information included various parameters such as age, gender, race, tumor stage, anatomical neoplastic division, smoking history, and more.

2.2 Criteria for selecting gut microbes and microbe target biomarkers

To identify gut microbes associated with LUAD, we employed a systematic approach. We first conducted differential abundance analysis on microbial data from LUAD patients and healthy controls using the Peryton and GutMGene databases, with DESeq2 as the analysis tool. The criteria for selecting differentially abundant microbes included an adjusted p-value < 0.05 and a log2 fold change (log2FC) > 1, ensuring statistical significance and biological relevance. We refined our selection by correlating microbe abundance with clinical outcomes like patient survival and disease progression, prioritizing microbes with significant correlations (p-value < 0.05). We focused on microbes with potential mechanistic roles in LUAD by using the GutMGene database to identify known interactions with human genes and metabolites relevant to cancer pathways. For the selection of 767 microbe target biomarkers, we retrieved mRNA transcriptome data from the TCGA database for LUAD samples and identified differentially expressed genes (DEGs) by comparing cancer tissues with adjacent normal tissues using the "limma" package in R. DEGs were selected based on an adjusted p-value < 0.05 and |log2FC|> 1. We mapped the DEGs to potential microbial targets using the GutMGene database, filtering associations based on known interactions with pathways implicated in cancer progression and immune modulation. Finally, we integrated data from microbial abundance analysis and gene expression profiling to identify targets consistently associated with both microbial changes and gene expression alterations in LUAD. This comprehensive approach enabled us to identify 150 gut microbes and 767 microbe target biomarkers with potential relevance to LUAD pathogenesis and prognosis.

2.3 Gene expression analysis

For gene expression analysis, we employed R v3.6.1 software (https://www.r-project.org/) along with the "limma" package. We compared the expression data (HTseq-Counts) of KLF5 between adjacent tissues and cancer tissues. After excluding adjacent tissue samples, we identified DEGs based on the median KLF5 expression.

2.4 Enrichment analysis

To identify enriched pathways and functional sets, we conducted pathway enrichment analysis across cellular components (CC), Kyoto Encyclopedia of Genes and Genomes (KEGG), biological processes (BP), and molecular functions (MF) using the "ClusteProfiler" package in R. Additionally, we employed Gene Set Enrichment Analysis (GSEA) v4.0.3 software (www.gsea.com) for the analysis with 1000 iterations. The significantly enriched pathway sets were evaluated based on the false discovery rate (FDR) and p-value.

To investigate the potential mechanisms of KLF affecting LUAD prognosis, all tumor samples in the TCGA dataset were divided into low and high expression groups. The entire gene expression data of patients from different groups were then inputted into GSEA v4.0.3 software (www.gsea.com). We set the number of iterations to 1000 and selected KEGG pathways for enrichment analysis. Subsequently, we scored the enrichment pathways for various risk groups. A higher score indicated significant enrichment in the high-risk group, while a lower score indicated significant enrichment in the low-risk group.

2.5 Immune infiltration analysis

For immune infiltration analysis, we utilized the GSVA package to perform single-specimen gene set enrichment analysis (ssGSEA) [21]. This analysis allowed us to calculate 24 immune infiltration scores for each sample. The markers for these 24 immune cells were sourced from a publication on immunity [22]. Gene data were obtained from the TCGA database (https://portal.gdc.cancer.gov/). The LUAD project utilized RNAseq data in Level 3 HTSeq fragments per kilobase of transcript per million mapped reads (FPKM) format. The FPKM data were transformed into transcripts per million reads (TPM) format, followed by log2 conversion. These immune infiltration scores were then used to investigate the relationship between KLF5 expression and the distribution with low and high KLF5 expression.

2.6 Protein–protein interactions (PPI) network

The PPI network of the DEGs was analyzed using the Search Tool for the Retrieval of Interacting Genes (STRING) database (http://string-db.org) [23]. Furthermore, hub genes were identified using MCODE (version 1.6.1) and the Cytoscape software (version 3.9.0), allowing for the mapping and visualization of the network.

2.7 Correlation of KLF5 expression and clinic pathological characteristics

The distribution of KLF5 expression was analyzed among subjects with different clinicopathological features. Kaplan–Meier analysis was employed to validate the relationship between KLF5 expression and individual survival time. Multivariate and univariate analyses were conducted to determine the indicators associated with patient survival. A nomogram was developed to predict clinical outcomes in cases with varying characteristics. The specificity and sensitivity of the nomogram were assessed using receiver operating characteristic (ROC) curves and relevant indexes.

2.8 Statistical analysis

All statistical analysis was performed using Python v3.9 and R v3.6.1 software. The Wilcoxon nonparametric test was used to determine differences between various tissues or KLF5 expression groups. The Pearson correlation test was employed to assess the relationship between KLF5 expression and clinicopathological characteristics of LUAD. Kaplan–Meier analysis was utilized to examine the association between KLF5 expression level and survival time. Statistical significance was considered at a p-value below 0.05, unless otherwise stated.

3 Results

3.1 Experimentally validated relationship among lung *cancer*, gut microbes, and KLF5

A hierarchical diagram illustrating the relationship between microorganisms and diseases was obtained from the Peryton database. We identified a total of 4065 cancer-related associations. Microorganisms related to diseases were categorized by genus, species, family, order, class, and phylum, resulting in the identification of 1747, 1110, 654, 284, 203, and 153 disease-related microorganisms, respectively. Additionally, we found 88 microorganisms related to lung cancer categorized by genus, species, family, order, class, and phylum, with the counts being 20, 17, 11, 5, and 9, respectively. All data

are obtained from the experimentally verified online database peryton at https://dianalab.e-ce.uth.gr/peryton/#/microdishier.

In the Peryton dataset, a graph network depicts the relationship between microorganisms and lung neoplasms (Fig. 2A). Experimentally validated microorganisms associated with lung neoplasms include *Firmicutes, Bifidobacterium, Streptococcus, Clostridium, Veillonella, Actinobacteria, Selenomonas, Actinetobacter, Rothia*, and others. The chord diagram illustrates the phyla related to lung neoplasms (Fig. 2B). The experimentally validated phyla of microorganisms associated with lung neoplasms include *Actinetobacteria, Bacteroidetes, Candidatus Parcubacteria, Firmicutes, Fusobacteria, Proteobacteria, Spirochaetes, Synergistetes, and Tenericutes*. In the gut microbiota of lung cancer patients, the relative abundance of Faecalibacterium is significantly decreased compared to healthy populations.

Furthermore, a novel relationship network diagram among lung cancer, gut microbes, and KLF5 was identified through the gutMGene database using Gephi in Python. KLF5 in the gut of patients with lung cancer is directly or indirectly down-regulated by *Akkermansia muciniphila* and *Faecalibacterium prausnitzii*, potentially through metabolite targeting, such as butyrate (Fig. 2C, D). Butyrate, a metabolic product of *Faecalibacterium prausnitzii*, can inhibit intestinal KLF5 expression, while *Akkermansia muciniphila* is capable of directly inhibiting intestinal KLF5 expression.

3.2 The expression of KLF5 in tumors contrasted with normal specimens

To elucidate the role of KLF5 in LUAD tumorigenesis, we conducted a comparative analysis of its expression and distribution in LUAD and other cancer types. RNAseq data in TPM format were utilized for analysis after log2 conversion. In the TCGA dataset, KLF5 was significantly overexpressed in various tumors, including LUAD (Fig. 3A). Importantly, the expression level of KLF5 in cancer tissues was significantly higher compared to adjacent tissues ($p < 0.01$) (Fig. 3B).

A total of 1593 DEGs were identified from gene expression RNA-seq-HTSeq-Counts data, satisfying the threshold of $|\log2(FC)| > 1$. Among these, 769 genes were found to be up-regulated, while 824 genes were down-regulated in cancer patients (Fig. 3C). The DEGs were then further screened based on a significance threshold of $p < 0.05$, and the top 10 positively and negatively correlated genes were selected. KLF5 is significantly correlated with the 20 DEGs, as shown in the Fig. 3D.

3.3 Functional enrichment analysis of DEGs

To further investigate the functions of KLF5-associated DEGs in LUAD, we utilized Metascape to perform Gene Ontology (GO) and KEGG enrichment analysis. The results revealed significant enrichments of KLF5-associated DEGs in various categories, including epidermis development, apical part of the cell, peptidase regulator activity, intermediate filament cytoskeleton, intermediate filament, enzyme inhibitor activity, endopeptidase regulator activity, endopeptidase inhibitor activity, chemical carcinogenesis, and peptidase inhibitor activity. Additionally, pathways such as Xenobiotics Metabolism by cytochrome P450 and Drug metabolism-cytochrome P450 were also found to be involved in the regulation of KLF5-interacting genes (Fig. 4A–D, Supplementary Table 1–4).

GSEA was employed to identify critical signaling pathways associated with LUAD by comparing datasets with low and high KLF5 expression. In the low KLF5 subgroup, pathways such as CD22-MEDIATED-BCR regulation, IMMUNOREGULATORY interactions, LAT2-NTAL-LAB-ON-CALCIUM mobilization, CREATION-OF-C4-AND-C2 activators, and PHOSPHOLIPIDS-IN-PHAGOCYTOSIS were significantly enriched with adjusted FDR values < 0.05 (Fig. 5A–E). In contrast, pathways including XENOBIOTICS-BY-CYTOCHROME-P450, DRUG-METABOLISM-CYTOCHROME-P450, RETINOL-METABOLISM, COMPOUNDS, and CORNIFIED-ENVELOPE were significantly enriched in the high KLF5 subgroup (Fig. 5F–J).

3.4 Immune infiltration analysis associated and PPI network in LUAD

The expression of KLF5 was found to be associated with immune infiltration in the LUAD microenvironment with 24 immune cell subsets showing correlations with KLF5 expression, including 4 subsets with positive correlations and 20 subsets with negative correlations (Fig. 6A, B). The size of the dots represents the absolute value of Spearman's correlation coefficient (r). Specifically, KLF5 was strongly associated with the infiltration of central memory T (Tcm) cells and negatively correlated with the infiltration of Th1 cells (Fig. 6C–F). These findings suggest that KLF5 may play a role in regulating the tumor immune landscape in LUAD.

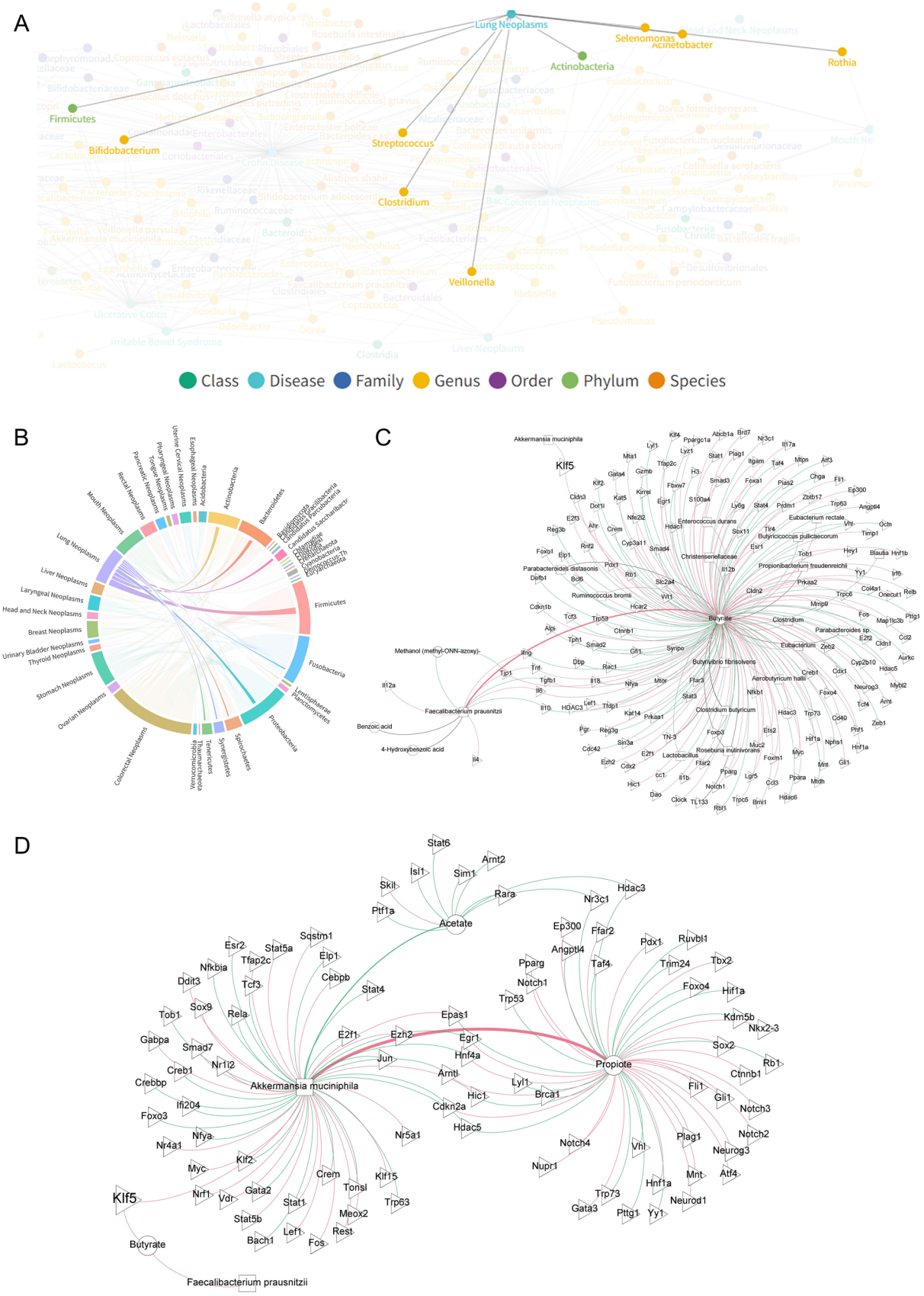

Fig. 2 Association map of microorganisms and Lung cancer. **A** The relationship between microorganisms and lung neoplasms. **B** Phylum of microorganisms associated with lung neoplasms. **C**, **D** Network diagram of the relationship among lung cancer, gut microbes, and KLF5

Fig. 3 Expression and analysis of KLF5 in tumors compared to normal specimens. **A** KLF5 expression levels in paired normal and pan-cancer specimens, indicating significant overexpression in various tumors, including LUAD. **B** Comparison of KLF5 expression levels in paired normal and LUAD specimens, showing significantly higher expression in cancer tissues ($p < 0.01$). **C** Volcano plot illustrating the differentially expressed genes (DEGs) between LUAD and normal tissue samples. The plot highlights genes with significant changes in expression, with upregulated genes shown in red and downregulated genes in green. DEGs were identified using a threshold of $|\log2(FC)| > 1$ and a p-value < 0.05. **D** Heat map of the top 20 genes positively and negatively correlated with KLF5 expression, providing insights into potential co-expressed genes and pathways

The STRING platform was utilized to construct the network of KLF5 and its potential co-expressed genes among the KLF5-associated DEGs. After filtering out DEGs with |log fold change (logFC)|> 1.5 and p-value < 0.05, a PPI network consisting of 111 nodes and 200 edges was visualized using Cytoscape-MCODE (Fig. 6G). The network displays the connections between KLF5 and its 22 potential co-interactions (Fig. 6H).

3.5 Correlation between clinic pathological characteristics and KLF5 expression

Clinical data from 535 LUAD patients, with a median age of 56.7 years, including TNM staging, are presented in Table 1. KLF5 expression was observed to be low in 267 LUAD patients and high in the remaining 268 cases. The Fisher's exact test revealed a significant association between KLF5 expression and age group ($p = 0.003$). Logistic regression analysis demonstrated significant associations between KLF5 and pathological staging ($p = 0.039$) as well as anatomic neoplasm subdivision ($p = 0.013$) (Table 2). The area under the curve (AUC) for KLF5 was 0.753, indicating its potential as a robust biomarker for LUAD (Fig. 7A). Furthermore, the Wilcoxon rank-sum test showed significant associations between KLF5 expression and gender ($p < 0.01$), race ($p < 0.001$), disease specific survival (DSS) event, progression free interval (PFI) event, and overall survival (OS) event ($p < 0.001$) (Fig. 7B–F). Kaplan–Meier analysis and forest plot analysis of KLF5's prognostic value in LUAD revealed that individuals with high KLF5 expression were associated with poor OS (Figs. 7G, 8A). Moreover, the Kaplan–Meier analysis confirmed that high KLF5 expression was associated with poor prognosis in the M0 stage, and R0 patients (Fig. 7H, I).

3.6 Prognostic model of KLF5 in LUAD

In the following Cox regression models, variables with a p-value less than 0.1 are considered significant. The analysis revealed that KLF5 expression had a significant impact on T2 (HR = 1.521 (1.068–2.166), $p = 0.02$), T3 and T4 (HR = 3.066 (1.950–4.823, $p < 0.001$), N1 (HR = 2.382 (1.695–3.346, $p < 0.001$), N2 and N3 (HR = 2.968 (2.040–4.318, $p < 0.001$), M1 (HR = 2.136 (1.248–3.653), $p < 0.001$), Stage II (HR = 2.418 (1.691–3.457, $p < 0.001$), Stage III (HR = 3.544 (2.437–5.154, $p < 0.001$), Stage IV (HR = 3.790 (2.193–6.548, $p < 0.001$), R1 (HR = 3.255 (1.694–6.251, $p < 0.001$), and R2 (HR = 11.085 (3.443–35.689, $p < 0.001$). Importantly, the high expression of KLF5 was associated with poor OS (HR = 1.354 (1.014–1.809), $p = 0.04$) (Table 3). Consistently, the forest plot revealed that KLF5 overexpression predicted poor prognosis in various LUAD subtypes (Fig. 8A).

Utilizing the RMS R program, a nomogram was developed based on the results of the Cox regression analysis to predict the prognosis of LUAD patients more accurately (Fig. 8B). The TNM stage, primary therapeutic outcome, residual tumor, and KLF5 expression were incorporated as independent prognostic factors in the model. By drawing a line from the overall score axis down to the survival outcome axis, the probability of 1, 5, and 15-year survival in LUAD patients could be calculated. Notably, under the same conditions, high expression of KLF5 predicted a shorter survival rate. The calibration curve of the nomogram for OS demonstrated overall agreement between the predicted and observed outcomes in all patients (Fig. 8C).

4 Discussion

For a long time, the early diagnosis of lung adenocarcinoma has been challenging due to the absence of typical symptoms and sensitive biomarkers. It is often diagnosed when severe symptoms manifest, leading to missed opportunities for surgical intervention [24]. Therefore, the identification of new prognostic biomarkers can greatly improve the prediction of survival and prognosis in patients with LUAD. In this study, we discovered a close relationship between non-small-cell

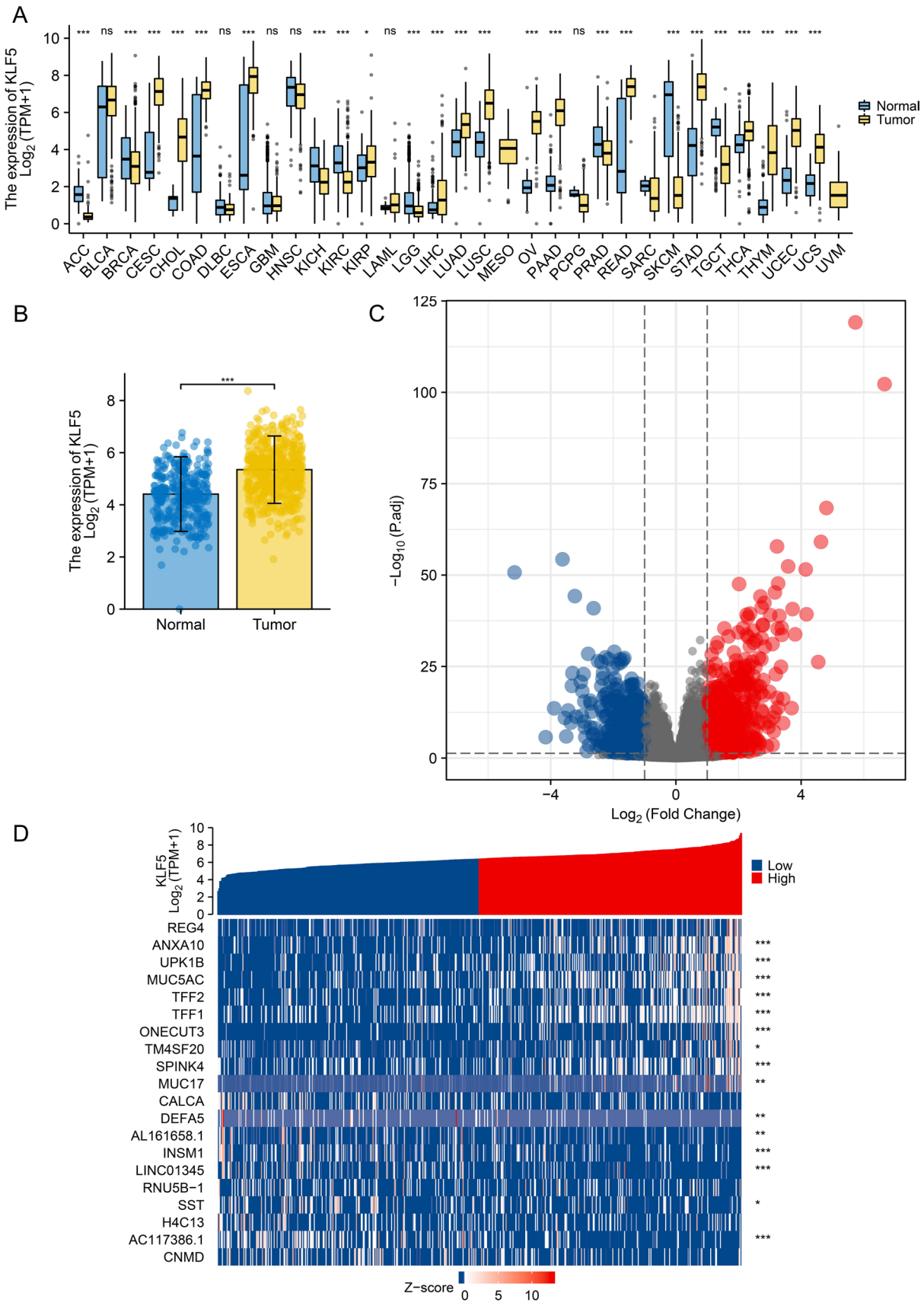
A
The expression of KLF5 Log2 (TPM+1)
Normal
Tumor
ACC BLCA BRCA CESC CHOL COAD DLBC ESCA GBM HNSC KICH KIRC KIRP LAML LGG LIHC LUAD LUSC MESO OV PAAD PCPG PRAD READ SARC SKCM STAD TGCT THCA THYM UCEC UCS UVM
B
The expression of KLF5 Log2 (TPM+1)
Normal
Tumor
C
−Log10 (P.adj)
Log2 (Fold Change)
D
KLF5 Log2 (TPM+1)
Low
High
REG4
ANXA10
UPK1B
MUC5AC
TFF2
TFF1
ONECUT3
TM4SF20
SPINK4
MUC17
CALCA
DEFA5
AL161658.1
INSM1
LINC01345
RNU5B−1
SST
H4C13
AC117386.1
CNMD
Z−score

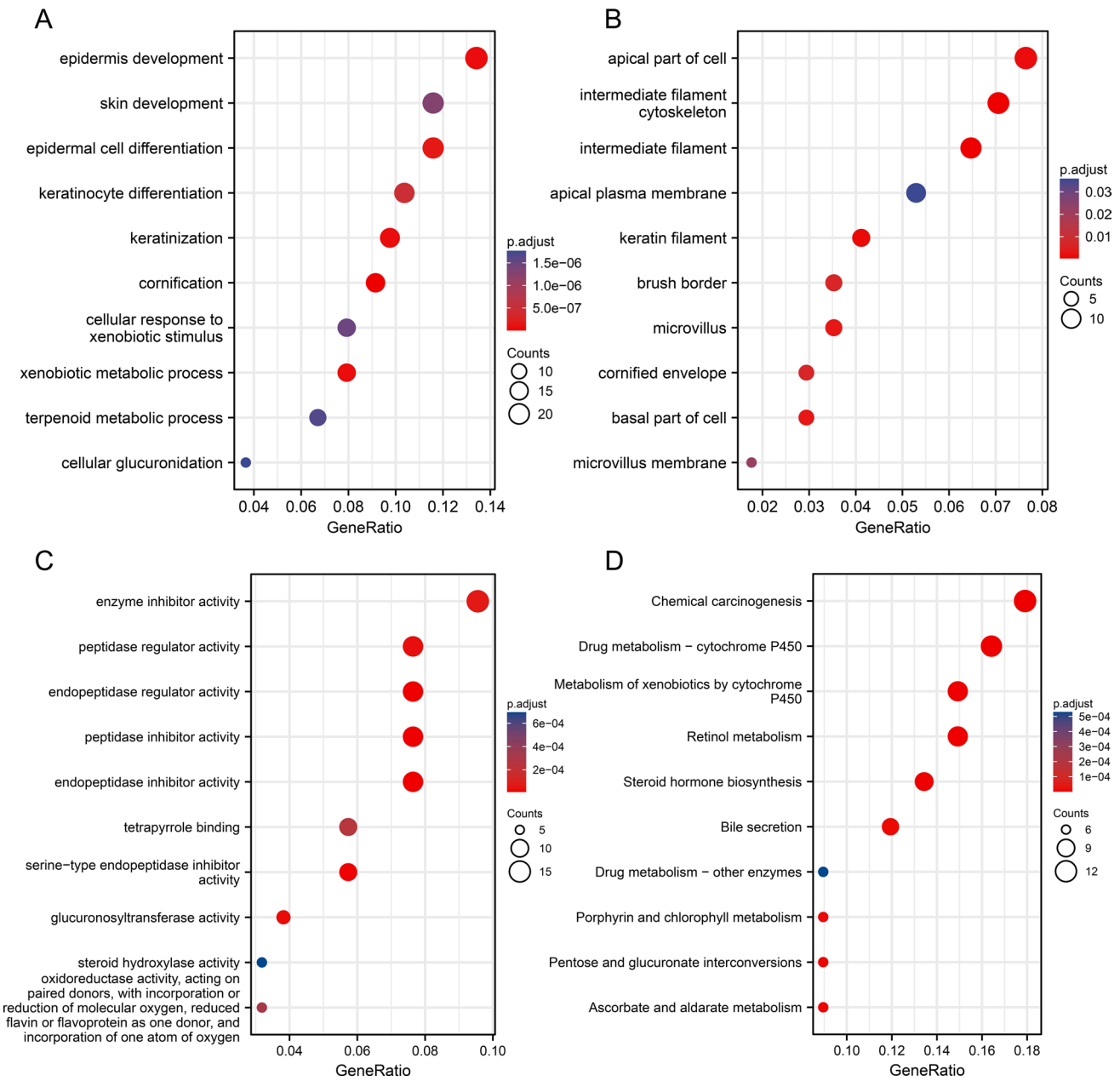

Fig. 4 KLF5 functional enrichment analysis. **A** Gene annotation map for biological processes in the cyan-colored module. **B** Gene annotation map for genes in the cyan-colored module. **C** Gene annotation map for cellular components in the cyan-colored module. **D** Genes' Annotation map in the cyan-colored module from the Genes and Genomes' Kyoto Encyclopedia

lung cancer (NSCLC), gut microbiota (metabolites), and intestinal KLF5 through the analysis of the Peryton and gutMGene databases. Building on the concept of the Gut-lung axis [10, 25–27], we observed a strong association between specific gut microbiota (*Akkermansia muciniphila* and *Faecalibacterium prausnitzii*) and their target gene KLF5 in lung cancer. *Akkermansia muciniphila* has been reported to induce intestinal adaptive immune responses in homeostasis [28] and gut *Akkermansia muciniphila* has been shown to predict the clinical response to PD-1 blockers in patients with advanced NSCLC [29]. Furthermore, NSCLC patients often exhibit gut dysbiosis characterized by a significant decrease

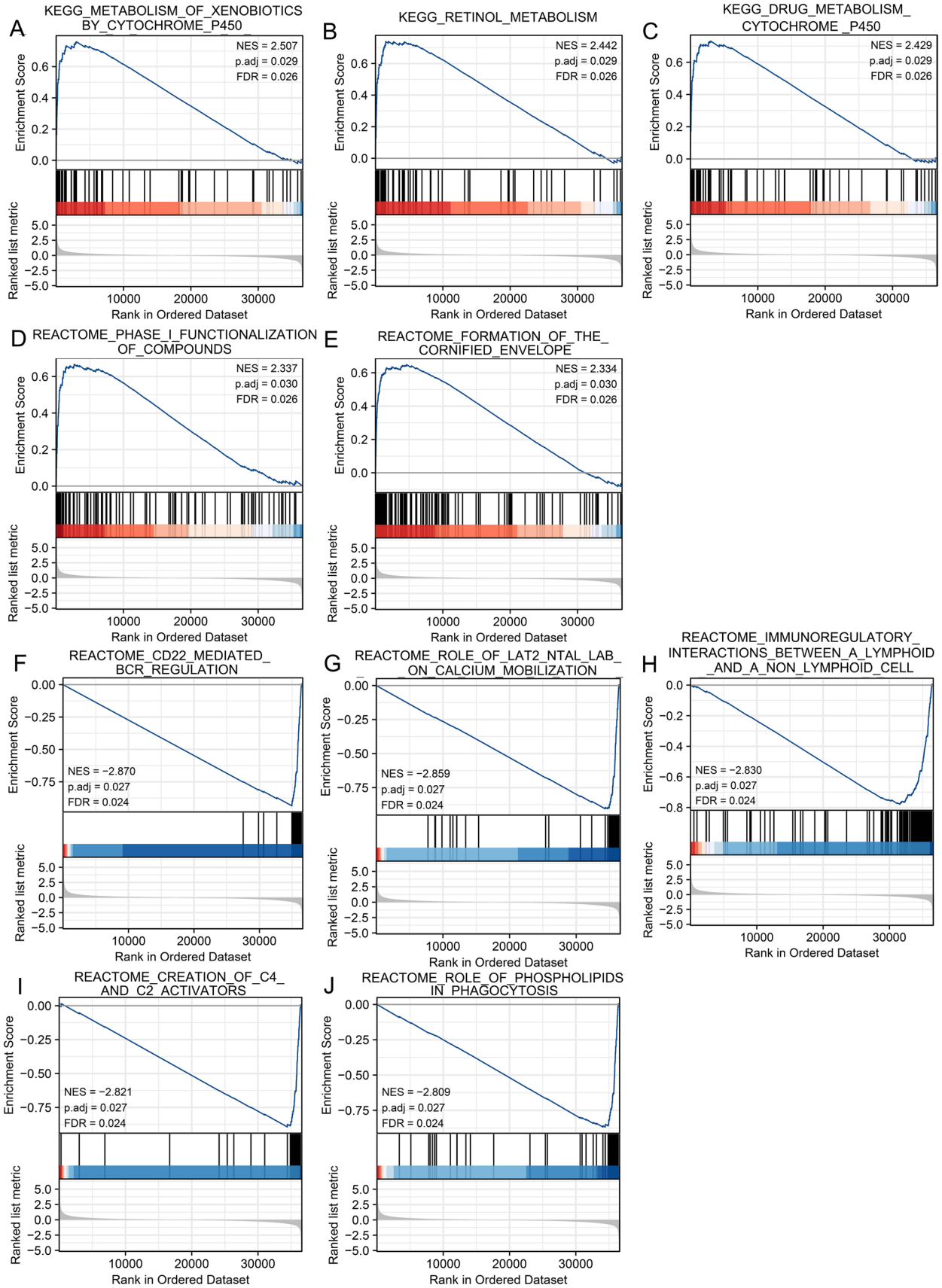

Fig. 5 KLF5-associated signaling pathways recognized by GSEA. **A**–**E** The KLF5 low subgroup. **F**–**J** The KLF5 high subgroup

Fig. 6 Results of analysis between immune infiltration and KLF5 expression. **A**, **B** Relation between the 24 immune cells' relative abundances and KLF5 expression level. **C**–**F** Tcm cells were considerably positively associated with KLF5 expression as well as infiltration level in various KLF5 expression groups and Th1 cells were inversely correlated with KLF5 expression and infiltration level in various KLF5 expression groups. **G** Cytoscape was used to build the DEG PPI network. **H** The KLF5 Network and prospective coexpression genes in KLF5-related DEGs

in butyrate-producing bacteria such as *Faecalibacterium prausnitzii* [30]. *Faecalibacterium prausnitzii*, known for its anti-inflammatory properties [31, 32], may play a role in the inflammatory cancer transformation of NSCLC.

The TCGA dataset from GSEA was employed in this study to investigate the role of KLF5 in LUAD and to provide insights for future research in this field. To account for heterogeneity in sequencing depth and gene length data, conversion to TPM (transcripts per million) was used to normalize the gene expression levels. This normalization procedure ensures that the impact of gene length, sequencing depth, and gene expression rate is minimized, allowing for meaningful comparisons of gene expression levels across different cells and conditions within the dataset. This standardized approach facilitates the analysis of gene expression patterns and comparisons of expression levels in LUAD.

Our findings demonstrate that KLF5 gene expression serves as a prognostic indicator for both OS and disease-free survival in LUAD. Through GSEA, we observed that low expression of KLF5 is associated with favorable prognostic factors such as CD22-MEDIATED-BCR regulation, LAT2-NTAL-LAB-ON-CALCIUM mobilization, IMMUNOREGULATORY interactions, CREATION-OF-C4-AND-C2 activators, and PHOSPHOLIPIDS-IN-PHAGOCYTOSIS. On the other hand, high expression of KLF5 is linked to pathways such as RETINOL-METABOLISM, XENOBIOTICS-BY-CYTOCHROME-P450, DRUG-METABOLISM-CYTOCHROME-P450, COMPOUNDS, and CORNIFIED-ENVELOPE. These findings suggest that KLF5 not only serves as a potential predictive biomarker in LUAD but also represents a possible therapeutic target as it influences key tumorigenesis pathways.

Our findings also revealed a significant positive correlation between KLF5 expression and Tcm cells, as observed in our immune cell infiltration analysis. Tcm cells are known to possess the ability to resist lymphoid cell proliferation and homing, and their function is highly dependent on the expression of the chemokine receptor (CCR)-7 and the lymphoid tissue-homing receptor CD62L [33]. This suggests that the overexpression of KLF5 may enhance the immune response and infiltration of Tcm cells during tumor progression.

In contrast, we observed an inverse association between KLF5 expression and Th1 cells. Th1 cells are primarily responsible for secreting cytokines such as TNF-α and other molecules involved in cellular immune responses, playing a crucial role in immune defense against exogenous pathogens and tumors. The downregulation of Th1 cells caused by KLF5 overexpression may disrupt the balance of Th1/Th2 cells, leading to an unfavorable prognosis. This is consistent with our Kaplan–Meier survival curve analysis, which demonstrated that patients with high KLF5 expression were associated with lower OS, DSS, and PFI. These findings suggest that KLF5 could serve as a potential prognostic biomarker in LUAD patients.

Furthermore, the Cox analysis conducted in our study suggests that KLF5 may serve as an independent predictor of poor prognosis in LUAD patients. Specifically, tumor status and high expression of KLF5 were identified as predictive indicators of decreased overall OS based on multivariate Cox regression analysis. To further enhance the prognostic prediction, we developed a KLF5-associated nomogram that can estimate the 1-, 5-, and 10-year survival probabilities for individuals with LUAD. The nomogram was validated using the log-rank test and calibration chart to ensure its reliability and accuracy in predicting patient outcomes. These findings underscore the potential of KLF5 as a prognostic marker and highlight the utility of the nomogram in clinical practice.

Despite the promising results, this study has several limitations that need to be addressed. Firstly, the sample size was relatively small, which may limit the generalizability of the findings. Future studies with larger cohorts are necessary to validate these results. Secondly, while bioinformatics analyses provided valuable insights, experimental validation is required to confirm the role of KLF5 in immune regulation and its impact on LUAD progression. Finally, incorporating additional clinical data, such as detailed patient medication history, could enhance our understanding of KLF5's specific role in LUAD pathogenesis. Addressing these limitations will be crucial for advancing our knowledge in this field and paving the way for further investigations.

In LUAD, accurately distinguishing between low-risk and high-risk patients based on tumor stage, pathological status, and tumor size alone is challenging. Therefore, additional prognostic factors are required to improve risk stratification. Our study demonstrates that high expression of the KLF5 gene is associated with a poor prognosis in individuals with lung adenocarcinoma. Moreover, our findings indicate that KLF5 serves as an independent prognostic parameter for OS in these patients. These results highlight the significance of incorporating KLF5 expression as a valuable prognostic factor to better predict patient outcomes in LUAD.

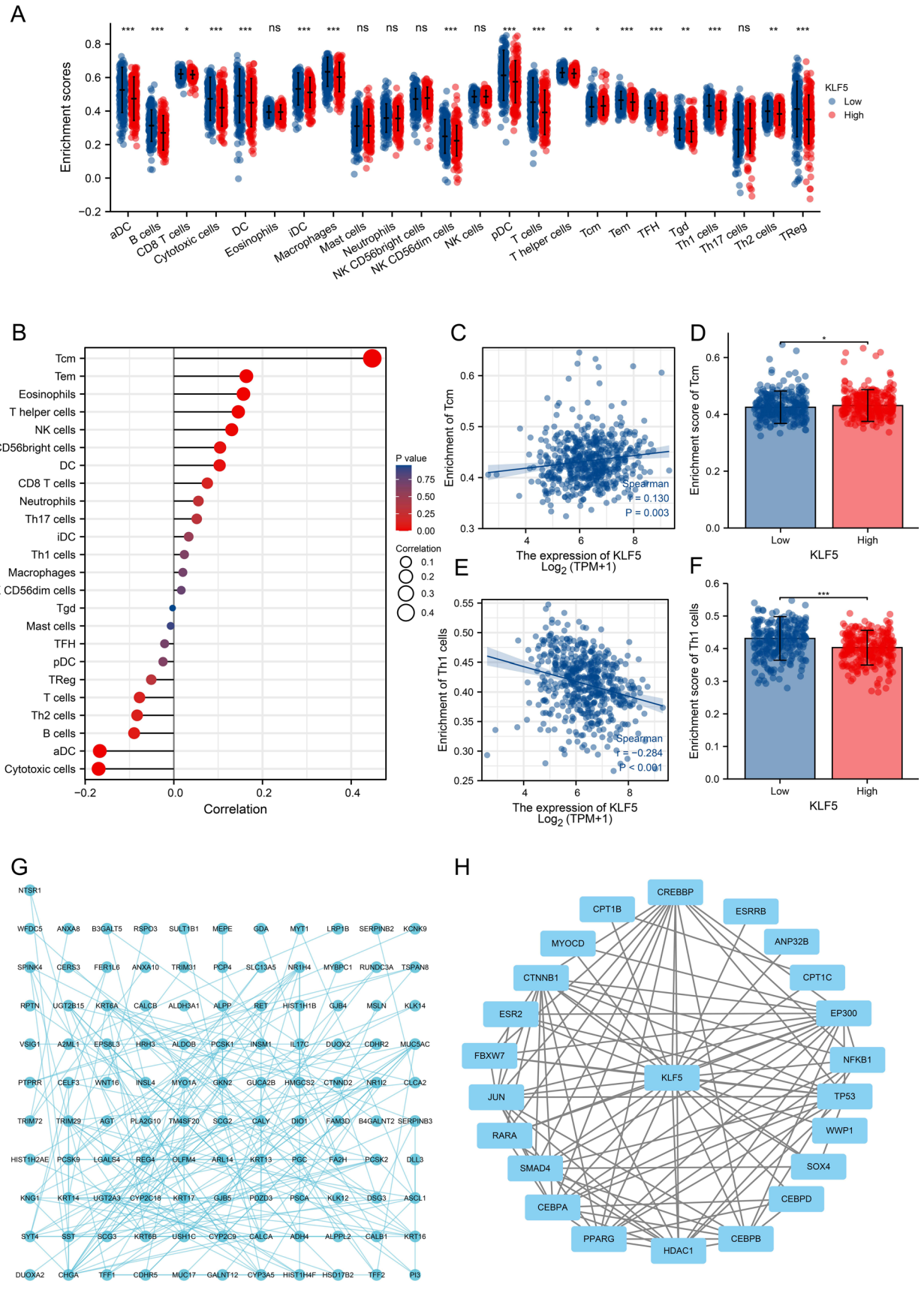
A
Enrichment scores
KLF5
Low
High
aDC
B cells
CD8 T cells
Cytotoxic cells
DC
Eosinophils
iDC
Macrophages
Mast cells
Neutrophils
NK CD56bright cells
NK CD56dim cells
NK cells
pDC
T cells
T helper cells
Tcm
Tem
TFH
Tgd
Th1 cells
Th17 cells
Th2 cells
TReg
B
P value
Correlation
Correlation
C
Enrichment of Tcm
The expression of KLF5 Log2 (TPM+1)
Spearman r = 0.130 P = 0.003
D
Enrichment score of Tcm
KLF5
E
Enrichment of Th1 cells
Spearman r = −0.284 P < 0.001
F
Enrichment score of Th1 cells
G
H
CREBBP
CPT1B
ESRRB
MYOCD
ANP32B
CTNNB1
CPT1C
ESR2
EP300
FBXW7
NFKB1
KLF5
JUN
TP53
RARA
WWP1
SMAD4
SOX4
CEBPA
CEBPD
PPARG
HDAC1
CEBPB

Table 1 Relation between clinicopathologic characteristics and KLF5 expression in LUAD specimens from the TCGA database

Characteristics	KLF5's low expression	KLF5's high expression	p-value
n	267	268	
T stage, n (%)			
T1	96 (18%)	79 (14.8%)	0.029
T2	145 (27.3%)	144 (27.1%)	
T3	21 (3.9%)	28 (5.3%)	
T4	4 (0.8%)	15 (2.8%)	
N stage, n (%)			
N0	176 (33.9%)	172 (33.1%)	0.152
N1	51 (9.8%)	44 (8.5%)	
N2	30 (5.8%)	44 (8.5%)	
N3	2 (0.4%)	0 (0%)	
M stage, n (%)			
M0	184 (47.7%)	177 (45.9%)	0.215
M1	9 (2.3%)	16 (4.1%)	
Age, median (IQR)	65 (58, 70)	67 (60, 74)	0.003

Table 2 KLF5 expression correlated with clinicopathological features (logistic regression)

Characteristics	Total (N)	Odds ratio (OR)	p value
T stage (T2 & T3 & T4 vs. T1)	532	1.337 (0.930–1.924)	0.117
N stage (N1 & N2 & N3 vs. N0)	519	1.085 (0.752–1.566)	0.663
M stage (M1 vs. M0)	386	1.848 (0.811–4.469)	0.153
Pathologic stage (Stage II & Stage IV vs. Stage I & Stage II)	527	1.567 (1.026–2.410)	0.039
Primary therapy outcome (SD & PR & CR vs. PD)	446	0.939 (0.565–1.564)	0.809
Race (White vs. Asian & Black or African American)	468	1.528 (0.893–2.646)	0.124
Gender (Male vs. Female)	535	1.322 (0.941–1860)	0.108
Age(> 65 Vs. < = 65)	516	1.282 (0.907–1813)	0.159
Residual tumor (R1 & R2 vs. R0)	372	1.157 (0.433–3.147)	0.769
Anatomic neoplasm subdivision (Right vs. Left)	520	0.638 (0.447–0.908)	0.013
Anatomic neoplasm subdivision2 (Peripheral Lung vs. Central Lung)	189	0.945 (0.509–1.744)	0.858
number_pack_years_smoked (≥ 40 vs. = 40)	369	0.851 (0.565–1.280)	0.438
Smoker (Yes vs. No)	521	0.923 (0.564–1.507)	0.749

Traditional Chinese medicine (TCM) makes a synergistic and attenuative effect when combined with chemoradiotherapy [34]. This study presents a potential connection between the TCM Theory of Exterior-Interior Correlation Between the Lung and Large Intestine and the concept of the Gut-lung axis [10, 11, 27, 35]. Building upon the emerging field of tumor microbiology, we propose the concept of TCM tumor microbiology, which encompasses the idea of tonifying yuan qi (primordial qi) and detoxification in the context of cancer treatment. This concept suggests that TCM treatment of cancer may involve the regulation of the microbiota-metabolism-immunity-inflammation-target gene axis, providing a potential scientific foundation for understanding the underlying principles of "strengthening vital qi to treat cancer", as advocated by TCM master Jiaxiang Liu. This perspective opens new avenues for investigating the mechanisms and potential benefits of TCM in cancer treatment.

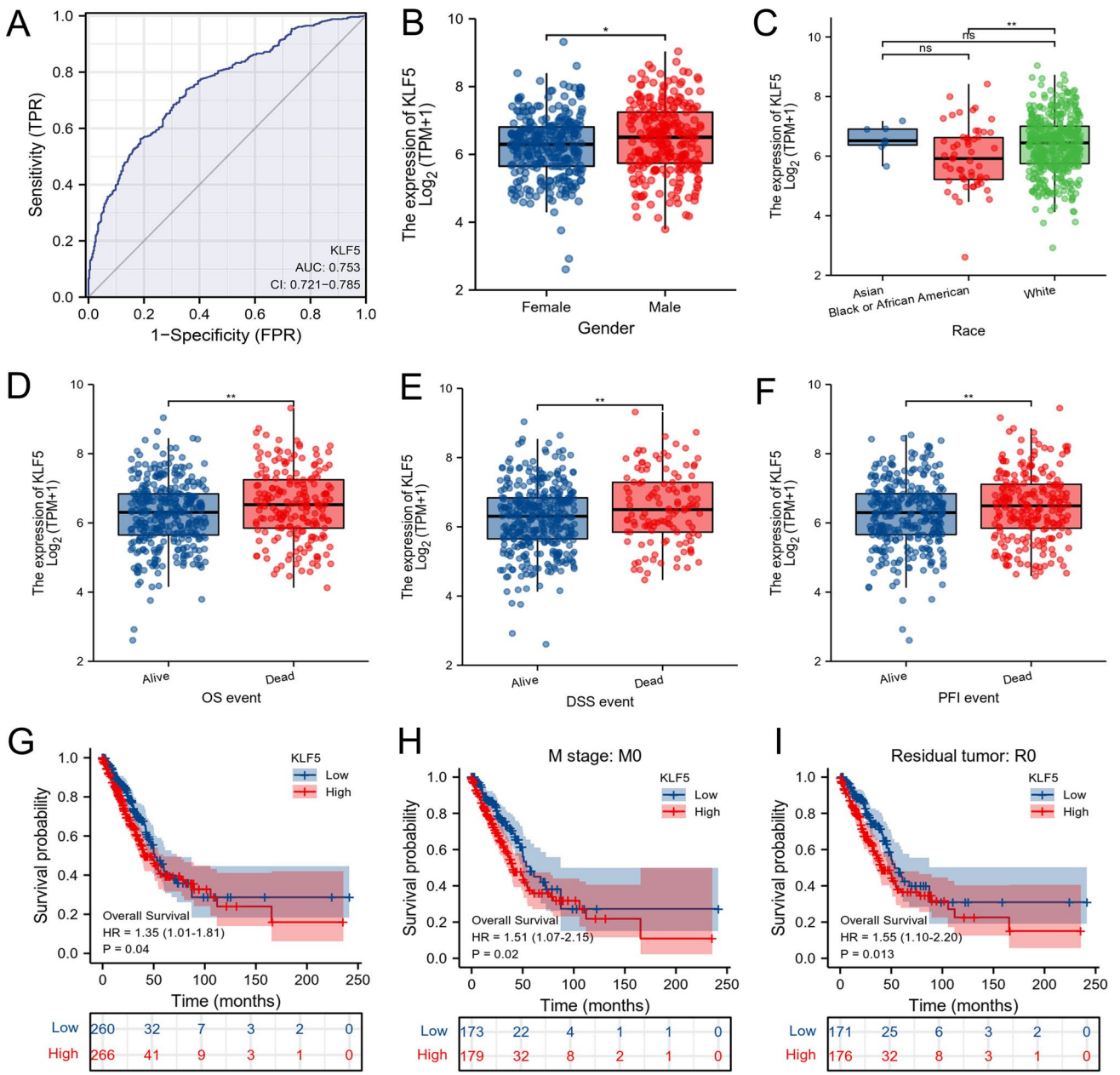

Fig. 7 Relationship between the expression of KLF5 and other clinicopathological traits. **A** ROC analysis was used to determine KLF5's diagnostic effectiveness in LUAD. **B**–**F** P56 is highly expressed in male, white, or patients with OS, DSS, and PFI events. **G**–**I** High expression of KLF5 in LUAD patients, M0 patients, and R0 patients suggests poor prognosis

While our study has provided valuable insights into the relationship between KLF5, gut microbiota, and LUAD, there are several limitations that need to be addressed. Firstly, the sample size in our study was relatively small. To enhance the robustness and generalizability of our findings, future research should include larger cohorts of patients. Secondly, experimental validation is needed to elucidate the precise role of KLF5 in immune regulation within LUAD. This would provide a more comprehensive understanding of the underlying mechanisms. Lastly, the inclusion of additional clinical factors, such as detailed patient medication information, would contribute to a better understanding of the specific role of KLF5 in the pathogenesis of LUAD. Addressing these limitations will contribute to the advancement of our knowledge in this field and pave the way for further investigations.

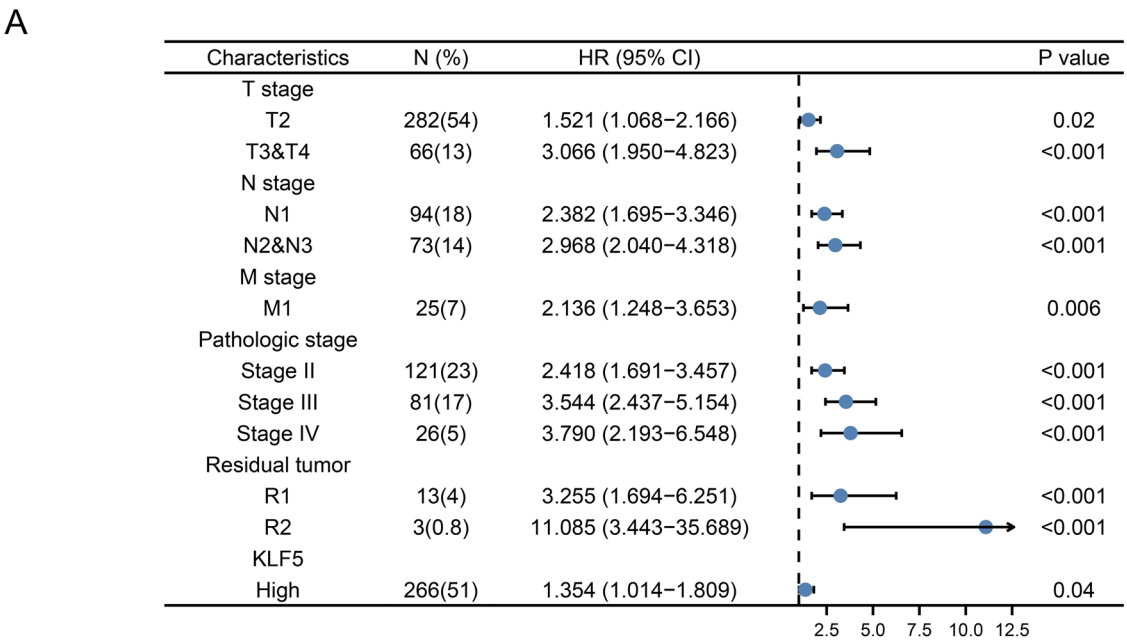

Fig. 8 KLF5 predictive and prognostic model in LUAD. **A** The predictive value of KLF5 in LUAD total survival is shown in the forest plot. **B** KLF5 predictive and prognostic model in LUAD Nomogram for estimating the likelihood of LUAD OS over 1, 5, and 10 years. **C** The nomogram's calibration plot is used to estimate the likelihood of OS at 1, 5, and 10 years

Table 3 Clinicopathological factors' multivariate and univariate analyses in individuals with LUAD

Characteristics	Total (N)	Univariate analysis		Multivariate analysis	
		Hazard ratio (95% CI)	p value	Hazard ratio (95% CI)	p value
T stage	523				
T1	175	Reference			
T2	282	1.521 (1.068–2.166)	**0.020**	1.117 (0.640–1.949)	0.696
T3	47	2.937 (1.746–4.941)	**<0.001**	3.193 (1.132–9.008)	**0.028**
T4	19	3.326 (1.751–6.316)	**<0.001**	2.203 (0.659–7.366)	0.200

Table 3 (continued)

Characteristics	Total (N)	Univariate analysis		Multivariate analysis	
		Hazard ratio (95% CI)	p value	Hazard ratio (95% CI)	p value
N stage	510				
N0	343	Reference			
N1	94	2.382 (1.695–3.346)	**< 0.001**	2.617 (0.962–7.117)	0.060
N2 & N3	73	2.968 (2.040–4.318)	**< 0.001**	3.066 (0.933–10.076)	0.065
M stage	377				
M0	352	Reference			
M1	25	2.136 (1.248–3.653)	**0.006**	1.221 (0.380–3.920)	0.738
Pathologic stage	518				
Stage I	290	Reference			
Stage II	121	2.418 (1.691–3.457)	**< 0.001**	0.592 (0.211–1.665)	0.320
Stage III	81	3.544 (2.437–5.154)	**< 0.001**	0.777 (0.202–2.998)	0.714
Stage IV	26	3.790 (2.193–6.548)	**< 0.001**		
Primary therapy outcome	439				
PR	5	Reference			
SD	37	0.432 (0.093–2.005)	0.284	0.228 (0.041–1.283)	0.094
PD	71	1.423 (0.345–5.875)	0.625	0.683 (0.152–3.065)	0.618
CR	326	0.384 (0.094–1.566)	0.182	0.149 (0.034–0.651)	**0.011**
Gender	526				
Female	280	Reference			
Male	246	1.070 (0.803–1.426)	0.642		
Race	468				
Asian	7	Reference			
Black or African American	55	1.408 (0.187–10.599)	0.740		
White	406	2.030 (0.284–14.519)	0.481		
Age	516				
≤ 65	255	Reference			
> 65	261	1.223 (0.916–1.635)	0.172		
Residual tumor	363				
R0	347	Reference			
R1	13	3.255 (1.694–6.251)	**< 0.001**	2.641 (0.940–7.418)	0.065
R2	3	11.085 (3.443–35.689)	**< 0.001**		
Anatomic neoplasm subdivision	512				
Left	200	Reference			
Right	312	1.037 (0.770–1.397)	0.810		
Anatomic neoplasm subdivision2	182				
Central Lung	62	Reference			
Peripheral Lung	120	0.913 (0.570–1.463)	0.706		
number_pack_years_smoked	363				
< 40	183	Reference			
≥ 40	180	1.073 (0.753–1.528)	0.697		
Smoker	512				
No	72	Reference			
Yes	440	0.894 (0.592–1.348)	0.591		
KLF5	526				
Low	260	Reference			
High	266	1.354 (1.014–1.809)	**0.040**	1.222 (0.771–1.937)	0.394

5 Conclusion

Our study identifies KLF5 as a promising prognostic biomarker in LUAD through its association with gut microbiota and immune modulation. We highlighted 150 gut microbes and 767 microbial target biomarkers related to LUAD, with KLF5 overexpression linked to poor prognosis and alterations in the tumor immune microenvironment. While these findings suggest new avenues for therapeutic intervention, experimental validation is needed to confirm KLF5's role and mechanistic pathways in LUAD. Future research should focus on clinical validation and explore the potential of targeting KLF5 to improve patient outcomes, advancing our understanding of its role in LUAD progression and its integration into personalized treatment strategies.

Acknowledgements We would like to express our gratitude to the Home for Researchers platform for providing access to create the Figures in this study.

Author contributions Experimental design: CSD, QLS and MXZ; Experimental data: QLF, MJX, WYY and RXW; Study materials: NL, RQH, SK and AS; Data analysis: SSG, JLZ and XQS; Writing-original draft: QLF, MJX, WYY, QLS and CSD. All authors reviewed the manuscript.

Funding This work was supported in part by A special clinical research initiative for the health business, sponsored by the Shanghai Municipal Health Commission (No. 202040155); Xinglin Youth Talent Training System of Shanghai University of Traditional Chinese Medicine Xinglin Young Scholars (No. RC-2017-02-02); Shanghai Municipal Science and Technology Commissions Special Biomedical Technology Support Plan (No. 20S31904100); 2022 Shanghai University of Traditional Chinese Medicine emergency response to COVID-19 (No. 2022YJ-49); Key Discipline Program of the Shanghai Pudong New Area Health Commission (No. PWZxk2022-13); Talents Training Program of the Seventh People's Hospital, Shanghai University of Traditional Chinese Medicine (No. XX2021-14) and supplied by Talents Training Program of the Seventh People's Hospital, Shanghai University of Traditional Chinese Medicine (No. BDX2020-01); Shanghai Clinical Research Center of Traditional Chinese Medicine Oncology, Science and Technology Commission of Shanghai Municipality (21MC1930500).

Data availability Sequence data that support the findings of this study have been deposited in TCGA database and are available at the following URL: https://www.cancer.gov/ and https://xenabrowser.net/datapages/. Microbial data that support the findings of this study have been deposited in Peryton database and GutMGene database, and are available at the following URL: https://dianalab.e-ce.uth.gr/peryton/ and http://bio-annotation.cn/gutmgene/home.dhtml.

Declarations

Ethics approval and consent to participate Not applicable as the research conducted in this study did not involve direct interactions with human subjects or the collection of primary data.

Consent for publication All authors read the guidelines of the journal and agreed with consent for publication.

Competing interests The authors declare no competing interests.

Open Access This article is licensed under a Creative Commons Attribution-NonCommercial-NoDerivatives 4.0 International License, which permits any non-commercial use, sharing, distribution and reproduction in any medium or format, as long as you give appropriate credit to the original author(s) and the source, provide a link to the Creative Commons licence, and indicate if you modified the licensed material. You do not have permission under this licence to share adapted material derived from this article or parts of it. The images or other third party material in this article are included in the article's Creative Commons licence, unless indicated otherwise in a credit line to the material. If material is not included in the article's Creative Commons licence and your intended use is not permitted by statutory regulation or exceeds the permitted use, you will need to obtain permission directly from the copyright holder. To view a copy of this licence, visit http://creativecommons.org/licenses/by-nc-nd/4.0/.

References

1. Siegel RL, Miller KD, Wagle NS, Jemal A. Cancer statistics, 2023. CA Cancer J Clin. 2023;73(1):17–48. https://doi.org/10.3322/caac.21763.
2. Zhou L, Dong C, Xu Z, et al. NEDD8-conjugating enzyme E2 UBE2F confers radiation resistance by protecting lung cancer cells from apoptosis. J Zhejiang Univ Sci B. 2021;22(11):959–65. https://doi.org/10.1631/jzus.B2100170.
3. Hirsch FR, Scagliotti GV, Mulshine JL, et al. Lung cancer: current therapies and new targeted treatments. Lancet. 2017;389(10066):299–311. https://doi.org/10.1016/S0140-6736(16)30958-8.
4. Zhang Z, Dong C, Yu G, et al. Smart and dual-targeted BSA nanomedicine with controllable release by high autolysosome levels. Colloids Surf B Biointerfaces. 2019;182: 110325. https://doi.org/10.1016/j.colsurfb.2019.06.055.
5. Fitzgerald RC, Antoniou AC, Fruk L, Rosenfeld N. The future of early cancer detection. Nat Med. 2022;28(4):666–77. https://doi.org/10.1038/s41591-022-01746-x.
6. Sepich-Poore GD, Zitvogel L, Straussman R, Hasty J, Wargo JA, Knight R. The microbiome and human cancer. Science. 2021;371(6536):eabc4552. https://doi.org/10.1126/science.abc4552.

7. Chen Y, Zhang Y, Wang Z, et al. CHST15 gene germline mutation is associated with the development of familial myeloproliferative neoplasms and higher transformation risk. Cell Death Dis. 2022;13(7):586. https://doi.org/10.1038/s41419-022-05035-w.
8. Helmink BA, Khan MAW, Hermann A, Gopalakrishnan V, Wargo JA. The microbiome, cancer, and cancer therapy. Nat Med. 2019;25(3):377–88. https://doi.org/10.1038/s41591-019-0377-7.
9. Garrett WS. Cancer and the microbiota. Science. 2015;348(6230):80–6. https://doi.org/10.1126/science.aaa4972.
10. Mjösberg J, Rao A. Lung inflammation originating in the gut. Science. 2018;359(6371):36–7. https://doi.org/10.1126/science.aar4301.
11. Chakradhar S. A curious connection: teasing apart the link between gut microbes and lung disease. Nat Med. 2017;23(4):402–4. https://doi.org/10.1038/nm0417-402.
12. Gao Y, Li D, Liu YX. Microbiome research outlook: past, present, and future. Protein Cell. 2023;14(10):709–12. https://doi.org/10.1093/procel/pwad031.
13. Methatham T, Nagai R, Aizawa K. A new hypothetical concept in metabolic understanding of cardiac fibrosis: glycolysis combined with TGF-β and KLF5 signaling. Int J Mol Sci. 2022;23(8):4302. https://doi.org/10.3390/ijms23084302.
14. Zhao P, Sun J, Huang X, et al. Targeting the KLF5-EphA2 axis can restrain cancer stemness and overcome chemoresistance in basal-like breast cancer. Int J Biol Sci. 2023;19(6):1861–74. https://doi.org/10.7150/ijbs.82567.
15. Huang Q, Liu M, Zhang D, et al. Nitazoxanide inhibits acetylated KLF5-induced bone metastasis by modulating KLF5 function in prostate cancer. BMC Med. 2023;21(1):68. https://doi.org/10.1186/s12916-023-02763-4.
16. Jiang Z, Zhang Y, Cao R, et al. miR-5195-3p inhibits proliferation and invasion of human bladder cancer cells by directly targeting oncogene KLF5. Oncol Res. 2017;25(7):1081–7. https://doi.org/10.3727/096504016X14831120463349.
17. Luo Y, Chen C. The roles and regulation of the KLF5 transcription factor in cancers. Cancer Sci. 2021;112(6):2097–117. https://doi.org/10.1111/cas.14910.
18. Skoufos G, Kardaras FS, Alexiou A, et al. Peryton: a manual collection of experimentally supported microbe-disease associations. Nucleic Acids Res. 2021;49(D1):D1328–33. https://doi.org/10.1093/nar/gkaa902.
19. Cheng L, Qi C, Yang H, et al. gutMGene: a comprehensive database for target genes of gut microbes and microbial metabolites. Nucleic Acids Res. 2022;50(D1):D795–800. https://doi.org/10.1093/nar/gkab786.
20. Vivian J, Rao AA, Nothaft FA, et al. Toil enables reproducible, open source, big biomedical data analyses. Nat Biotechnol. 2017;35(4):314–6. https://doi.org/10.1038/nbt.3772.
21. Hänzelmann S, Castelo R, Guinney J. GSVA: gene set variation analysis for microarray and RNA-seq data. BMC Bioinformatics. 2013;14:7. https://doi.org/10.1186/1471-2105-14-7.
22. Liu Y, Zhao S, Chen Y, et al. Vimentin promotes glioma progression and maintains glioma cell resistance to oxidative phosphorylation inhibition. Cell Oncol (Dordr). 2023;46(6):1791–806. https://doi.org/10.1007/s13402-023-00844-3.
23. Li J, Wu Z, Pan Y, et al. GNL3L exhibits pro-tumor activities via NF-κB pathway as a poor prognostic factor in acute myeloid leukemia. J Cancer. 2024;15(13):4072–80. https://doi.org/10.7150/jca.95339.
24. Zhang H, Shi Y, Ying J, et al. A bibliometric and visualized research on global trends of immune checkpoint inhibitors related complications in melanoma, 2011–2021. Front Endocrinol (Lausanne). 2023;14:1164692. https://doi.org/10.3389/fendo.2023.1164692.
25. Bowerman KL, Rehman SF, Vaughan A, et al. Disease-associated gut microbiome and metabolome changes in patients with chronic obstructive pulmonary disease. Nat Commun. 2020;11(1):5886. https://doi.org/10.1038/s41467-020-19701-0.
26. Wypych TP, Wickramasinghe LC, Marsland BJ. The influence of the microbiome on respiratory health. Nat Immunol. 2019;20(10):1279–90. https://doi.org/10.1038/s41590-019-0451-9.
27. Wypych TP, Pattaroni C, Perdijk O, et al. Microbial metabolism of L-tyrosine protects against allergic airway inflammation. Nat Immunol. 2021;22(3):279–86. https://doi.org/10.1038/s41590-020-00856-3.
28. Ansaldo E, Slayden LC, Ching KL, et al. *Akkermansia muciniphila* induces intestinal adaptive immune responses during homeostasis. Science. 2019;364(6446):1179–84. https://doi.org/10.1126/science.aaw7479.
29. Derosa L, Routy B, Thomas AM, et al. Intestinal *Akkermansia muciniphila* predicts clinical response to PD-1 blockade in patients with advanced non-small-cell lung cancer. Nat Med. 2022;28(2):315–24. https://doi.org/10.1038/s41591-021-01655-5.
30. Gui Q, Li H, Wang A, et al. The association between gut butyrate-producing bacteria and non-small-cell lung cancer. J Clin Lab Anal. 2020;34(8): e23318. https://doi.org/10.1002/jcla.23318.
31. Liu Y, Chen Y, Wang F, et al. Caveolin-1 promotes glioma progression and maintains its mitochondrial inhibition resistance. Discov Oncol. 2023;14(1):161. https://doi.org/10.1007/s12672-023-00765-5.
32. Miquel S, Leclerc M, Martin R, et al. Identification of metabolic signatures linked to anti-inflammatory effects of *Faecalibacterium prausnitzii*. MBio. 2015;6(2):e00300-e315. https://doi.org/10.1128/mBio.00300-15.
33. Konjar Š, Ficht X, Iannacone M, Veldhoen M. Heterogeneity of tissue resident memory T cells. Immunol Lett. 2022;245:1–7. https://doi.org/10.1016/j.imlet.2022.02.009.
34. Wu L, Zhu Y, Yuan X, et al. The efficacy and safety of Zengxiao Jiandu decoction combined with definitive concurrent chemoradiotherapy for unresectable locally advanced non-small cell lung cancer: a randomized, double-blind, placebo-controlled clinical trial. Ann Transl Med. 2022;10(14):800. https://doi.org/10.21037/atm-22-2814.
35. Chu N, Chan JCN, Chow E. Pharmacomicrobiomics in western medicine and traditional Chinese medicine in type 2 diabetes. Front Endocrinol (Lausanne). 2022;13: 857090. https://doi.org/10.3389/fendo.2022.857090.

Publisher's Note Springer Nature remains neutral with regard to jurisdictional claims in published maps and institutional affiliations.